

## Preparation of CaCO<sub>3</sub>-Based Biomineralized Polyvinylpyrrolidone–Carboxymethylcellulose Hydrogels and Their Viscoelastic Behavior

Rushita Shah,<sup>1</sup> Nabanita Saha,<sup>1,2</sup> Takeshi Kitano,<sup>1,2</sup> Petr Saha<sup>1,2</sup>

<sup>1</sup>Polymer Centre, Faculty of Technology, Tomas Bata University in Zlin, nam. T. G. Masaryka 275, Zlin 762 72, Czech Republic

<sup>2</sup>Centre of Polymer Systems, University Institute, Tomas Bata University in Zlin, Nad Ovcirnou 3685, 760 01 Zlin, Czech Republic

Correspondence to: N. Saha (E-mail: nabanitas@yahoo.com or nabanita@ft.utb.cz)

**ABSTRACT:** In the blend of natural and synthetic polymer-based biomaterial of polyvinylpyrrolidone (PVP) and carboxymethylcellulose (CMC), fabrication of CaCO<sub>3</sub> was successfully accomplished using simple liquid diffusion technique. The present study emphasizes the biomimetic mineralization in PVP–CMC hydrogel, and furthermore, several properties of this regenerated and functionalized hydrogel membranes were investigated. The physical properties were studied and confirmed the presence of CaCO<sub>3</sub> mineral in hydrogel by Fourier transform infrared spectroscopy and Scanning electron microscopy. Moreover, the absorptivity of water and mineral by PVP–CMC hydrogel was studied to determine its absorption capacity. Further, the viscoelastic properties (storage modulus, loss modulus, and complex viscosity) of mineralized and swelled samples (time: 5–150 min) were measured against angular frequency. It is interesting to know the increase of elastic nature of mineralized hydrogel filled with CaCO<sub>3</sub> maintaining the correlation between elastic property and viscous one of pure hydrogel. All these properties of biomineralized hydrogel suggest its application in biomedical field, like bone treatment, bone tissue regeneration, dental plaque and tissue replacement, etc. © 2013 Wiley Periodicals, Inc. *J. Appl. Polym. Sci.* **2014**, *131*, 40237.

**KEYWORDS:** biomimetic; swelling; functionalization of polymers; CaCO<sub>3</sub>; biomineralized hydrogel

Received 18 July 2013; accepted 30 November 2013

DOI: 10.1002/app.40237

### INTRODUCTION

Over the past decade, a number of applications of hydrogels including the polymeric ones have arisen because of their advantageous and potential properties, such as high water holding capacity, equilibrium swelling degree, flexibility because of their three-dimensional cross-linked structures, biodegradability and good biocompatibility.<sup>1–8</sup> Many natural and synthetic hydrogels are already reported as having potential biological applications and considered as promising material for tissue engineering, as scaffolds, bone-tissue, and dental transplants.<sup>4–9</sup> Further, inspired by natural biogenic minerals, many researchers have attempted to mimic natural biomineralization through organic–inorganic hybridization in order to develop a new material for medical applications.<sup>10,11</sup> Biomineralization occurs in specific micro-environment and is finely tuned by cells and specialized biomacromolecules that offer great advantage for specific cell–material interaction. Biominerals like teeth, bones, and shells have beautiful and functional structure that cannot be achieved artificially but by the osteogenic process, they introduced the process of biomineralization and have drawn the

attention to the next generation inorganic synthesis methodology<sup>12</sup> which makes it possible to prepare biomineralized polymeric material. Through mesocrystal theory, it is possible to understand the mechanism of biomineralization processes found in nature.<sup>7,8,10</sup>

A challenge in the field of biomineralization is identifying the appropriate *in vitro* model for its phenomenon. There exist several methods of forming organic–inorganic hybrid materials, which include thermally phase-induced separation, solvent casting / particle leaching, microsphere sintering, scaffold coating, etc.<sup>13</sup> With respect to scaffolds forming, as for materials, mineralization is generally required to incorporate the bioactive mineral like as calcium carbonate or calcium phosphate into a polymer matrix. It is reported that only powders of hydroxyapatite and  $\beta$ -trichlorophosphate have been used for bone-filling materials in clinical use.<sup>12</sup> These materials are highly bioactive and biodegradable, but they were mechanically unstable and flow out of surrounding tissue after long-term use. So it will be beneficial to utilize biomaterials having soft interface, strong and flexible structure.<sup>12</sup> Nature produces a wide variety of

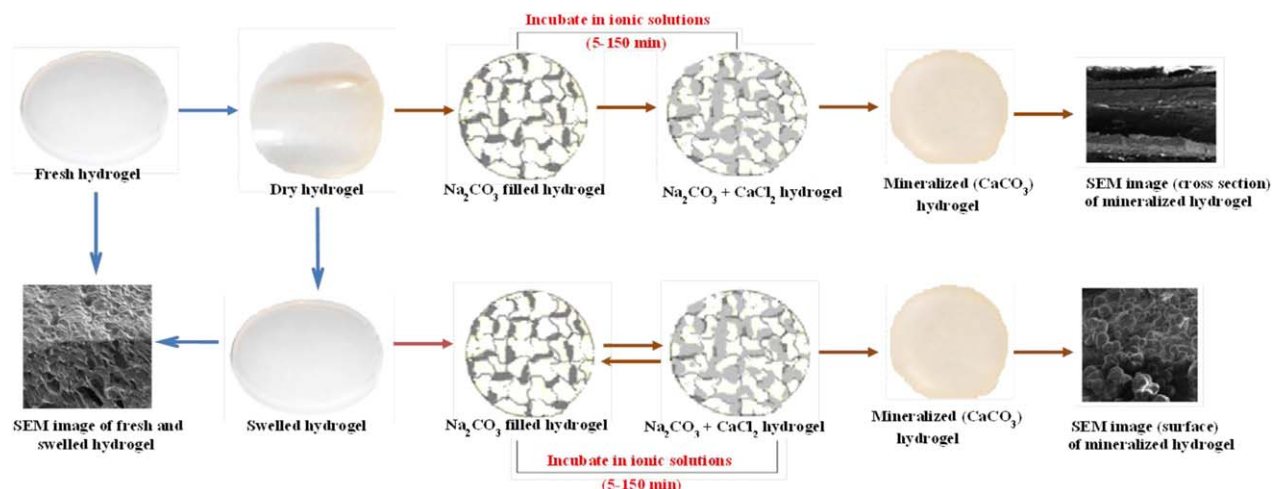


**Figure 1.** Schematic approach for the biom mineralization of PVP–CMC-based hydrogel. [Color figure can be viewed in the online issue, which is available at [wileyonlinelibrary.com](http://wileyonlinelibrary.com).]

attractive and highly functionalized mineralized tissues using simple inorganic salts. The well-known fascinating natural biomineral is calcium carbonate ( $\text{CaCO}_3$ ). This mineral exists in three different polymorphs of vaterite, aragonite, and calcite. Among them aragonite and calcite are mostly found as the polymorphs in natural system. All these polymorphs transform into most stable form, calcite, in presence of water.<sup>9,14–18</sup>

Several studies were carried out with template mediated mineralization using biological sources such as bacteria, algae, viruses, proteins, and biopolymers to obtain organic–inorganic composite hybrids. The matrix mediated mineralization process depends on the behavior and characteristic properties of extracellular matrix, which can be proteins, polysaccharides, or glycoproteins.<sup>19</sup> These matrices are often three-dimensional, fibrous, porous, and hydrated networks that can provide structural framework inorganic minerals to grow and so organic–inorganic hybrid composite materials or crystals can develop the materials with unique mechanical or structural properties. The growth of crystals in gels has emerged as a platform for biom mineralization process. Various gel matrices have been used as materials motivating the researchers to study in depth the interaction of gel like matrices in association with mineralization by biological organisms.<sup>16</sup> Till today, many matrices, for example alginate hydrogel,<sup>20</sup> agarose,<sup>21</sup> Poly(N-isopropylacrylamide-Co-Vinyl phosphonic acid),<sup>22</sup> bacterial cellulose,<sup>23</sup> and Polyvinyl alcohol,<sup>24</sup> have been used for carrying out mineralization process. Tomas Bata University in Zlin researchers have already developed a polysaccharide-based hydrogel termed “polyvinylpyrrolidone (PVP) and carboxymethylcellulose (CMC) hydrogel” applying a simple physical cross-linking agent (moist heat and pressure) without using any chemical cross-linking agents.<sup>3–6</sup> Thus, in this study it was decided to use a new biomaterial, PVP–CMC hydrogel, as an extracellular matrix for the preparation of  $\text{CaCO}_3$ -based biom mineralized scaffold. This calcite-based biomaterial will be useful for specific biomedical applications like bone tissue regeneration, enhancement of bone healing process, drug delivery, etc.

Moreover, among other interesting properties of hydrogels it is essential to know about viscoelastic behavior of biom mineralized

hydrogel. The viscoelastic properties depend on several intrinsic polymeric properties, nature of cross-linking, water content, as well as concentration of  $\text{CaCO}_3$  present in biom mineralized hydrogel.<sup>7,8</sup>

In this article, we describe the method of preparation of mineralized PVP–CMC hydrogel and its characterization in terms of physical appearance, physico-chemical structure, equilibrium swelling capacity in presence of water and equilibrium  $\text{CaCO}_3$  uptake capacity from ionic solutions, and their dynamic viscoelastic properties (storage modulus, loss modulus, and complex viscosity) of mineralized and swelled samples were measured against angular frequency under low strain amplitude.

## EXPERIMENTAL

Mineralized PVP–CMC hydrogel was prepared by simple liquid diffusion based technique<sup>7,8,10</sup> and it possesses several applications in the biomedical field. Then, characterization of the samples following standard method was done.

### Materials

PVP K30 (PVP: molecular weight 40,000), polyethylene glycol 3000 (PEG: average molecular weight 2700–3300) and agar were supplied by Fluka, Switzerland; carboxymethyl cellulose (CMC) was purchased from Sinopharm Chemical Reagent (SCRC), China; glycerin was obtained from Lachema, Czech Republic; calcium chloride ( $\text{CaCl}_2$ : molecular weight 110.99 g/mol, 97.0%), Penta, Czech Republic; sodium carbonate-10-hydrate ( $\text{Na}_2\text{CO}_3$ : molecular weight 286.14 g/mol) was obtained from Sigma Aldrich.

### Preparation of Biom mineralized Hydrogel

The biom mineralized hydrogel was prepared using ionic solution of calcium chloride ( $\text{CaCl}_2$ ) and sodium carbonate ( $\text{Na}_2\text{CO}_3$ ) by the following simple liquid diffusion technique as represented in Figure 1. The hydrophilic ‘PVP–CMC hydrogel’ was prepared following the solvent casting method applying only physical (moist heat and pressure) cross-linking agent.<sup>3–6</sup> The obtained fresh hydrogel was soft, smooth, off-white, and round (diameter 80 mm and thickness 6 mm). These fresh samples

were kept for 48–72 hrs at room temperature (22–25°C) for air drying as well as for freeze drying. The dry PVP–CMC hydrogel (diameter: 75 mm, thickness: 0.8–1.00 mm) was used for the preparation of biomineralized as well as water swelled PVP–CMC hydrogels. In the process of biomineralized hydrogel preparation, the dry PVP–CMC hydrogel was used as a matrix where  $\text{CaCl}_2 \cdot 2\text{H}_2\text{O}$  (14.7%, 1M, pH = 8.4) solution and  $\text{Na}_2\text{CO}_3$  (10.5%, 1M, pH = 7.4) solution were used (the concentration and pH of  $\text{CaCl}_2$  and  $\text{Na}_2\text{CO}_3$  solution was maintained as mentioned in Ref.<sup>10</sup>) as the source of  $\text{Ca}^{+2}$  and  $\text{CO}_3^{-2}$ , respectively. The dry hydrogel film first immersed in the 50 mL solution of  $\text{CaCl}_2 \cdot 2\text{H}_2\text{O}$  and then transferred into 50 mL  $\text{Na}_2\text{CO}_3$  solution. In this way, mineralization of  $\text{CaCO}_3$  in hydrogel matrix was carried out from 5 to 150 min keeping the test samples in each ionic solution for certain period and transferred them after equal incubation time interval. Finally, rubbery, round (diameter: 80 mm, thickness: 1–2 mm) and ivory hydrogels were obtained and designated as “mineralized hydrogel”.

Simultaneously, the dry PVP–CMC hydrogel was incubated in demineralized water at room temperature for the same duration. After a certain period (i.e. after 150 min), the water-soaked hydrogel became as good as a fresh hydrogel but the thickness of the water-soaked hydrogel sample varied with incubation period. The water-soaked hydrogel was termed as “swelled hydrogel”.

#### Scanning Electron Microscopy

The morphology of samples was determined by scanning electron microscopy (SEM). The SEM observation was carried out on VEGA II LMU (TESCAN) operating in the high-vacuum/secondary electron imaging mode at an accelerating voltage of 5–20 kV. The samples were sputter coated with a thin layer of palladium/gold alloy to improve the surface conductivity and tilted 30° for better observation. The images were taken at magnification of 100×–10k×.

#### Fourier Transform Infrared Spectroscopy

Fourier Transform Infrared Spectroscopy (FTIR) spectra of the specimens (Fresh PVP–CMC hydrogel and mineralized hydrogel) were obtained at wavenumber of 2000–600  $\text{cm}^{-1}$  at room temperature with uniform resolution of 2  $\text{cm}^{-1}$ . For this, attenuated total reflectance ATR-FTIR was used with NICOLET 320 FTIR Spectrophotometer with “Omnic” software package.

#### Study of Swelling Behavior

The degree of swelling of PVP–CMC hydrogel was investigated in the presence of water and ionic solutions ( $\text{Na}_2\text{CO}_3 + \text{CaCl}_2$ ) at room temperature (22–25°C) and swelling or mineralization time from 5 to 150 min.<sup>3,25,26</sup> The degree of swelling can be described by absorptivity of minerals and formation of  $\text{CaCO}_3$  in PVP–CMC hydrogel. The samples were immersed in mineral solutions until 150 min and in every specified time interval, the weight of the swelled and mineralized samples was recorded.

The swelling depends on absorptivity of water and formation of biogenic mineral within the hydrogel which is defined by eq. (1), wherein  $W_s$  and  $W_d$  are weights of the swollen and the dry PVP–CMC hydrogels, respectively. The PVP–CMC hydrogel is

swollen either because of absorption of  $\text{H}_2\text{O}$  and/or because of diffusion of ionic salts within the matrix which form  $\text{CaCO}_3$  crystal structure within the matrix as well as surface of the hydrogel:

$$\text{Absorptivity}\% = \left[ \frac{(W_s - W_d)}{W_d} \right] \times 100 \quad (1)$$

#### Measurement of Dynamic Viscoelastic Properties

The viscoelastic properties of hydrogels were examined by using a parallel plate rheometer testing device (ARES, Rheometrics Scientific, USA) and “TA Orchestrator” software for data evaluation. Dynamic frequency sweep tests were carried out at the temperature of 28°C to obtain the storage ( $G'$ - elastic part) and loss ( $G''$ - viscous part) moduli, and complex viscosity ( $\eta^*$ ). The geometry of measuring parallel plate was 25 mm in diameter, with a gap between plates depending on sample thickness (approximately 1–1.7 mm for mineralized, 1.8–6 mm for swelled hydrogel, and 6 mm for a fresh one). Measurement was conducted in oscillation mode with the frequency range from 0.1 to 100  $\text{rad s}^{-1}$  at 1% strain amplitude, which is considered as small strain amplitude to maintain the measurements within the linear viscoelastic region for homogeneous polymer substances. Influence of angular frequency and swelling time and mineralization time (time interval: 5–150 min) on  $G'$ ,  $G''$ , and  $\eta^*$ , which is calculated by the following equation of water swelled and mineralized hydrogel was discussed:

$$\eta^* = \sqrt{((G' \div \omega)^2 + (G'' \div \omega)^2)} \quad (2)$$

## RESULTS AND DISCUSSION

#### SEM Micrographs of Hydrogels

Figure 2 represents the SEM micrographs of pure PVP–CMC and biogenic mineralized (calcite) PVP–CMC hydrogels, which indicate both their surfaces and their cross-section structures. Figure 2(a) shows both structures of pure PVP–CMC hydrogel and gives the information of three-dimensional cross-linking network of hydrogel and the development of pores. In Figure 2(b–e), the surface and cross section of the hydrogels mineralized at different times are shown, and it is obvious that the granular shaped calcite crystals obtained by simple liquid diffusion technique are regenerated and accumulated continuously into the PVP–CMC hydrogel matrix. During the mineralization process the pores get filled up with  $\text{CaCO}_3$ . The fact that during the mineralization process the impregnated hydrogel membranes are incubated to ionic solutions of ( $\text{Na}_2\text{CO}_3 + \text{CaCl}_2$ ) is shown in Figure 1.  $\text{CaCO}_3$  accumulation is increased with respect to incubation time in ionic solution. Here, the  $\text{Ca}^{+2}$  ions are subjected to diffusion in the membrane and they act as nucleation sites for the carbonate mineralization. When the pores of PVP–CMC hydrogels are filled with  $\text{CaCO}_3$ , the nucleation of  $\text{Ca}^{+2}$  ions continuous on the surface of the hydrogel which is clearly visible at Figures 2(c,d,e).

#### FTIR Analysis of Hydrogels

The FTIR spectra of pure  $\text{CaCO}_3$ , calcite-based PVP–CMC hydrogel and nonmineralized PVP–CMC hydrogels are shown in Figure 3. From the spectrum some important characteristics can be described as follows: 1654  $\text{cm}^{-1}$  for C=O vibration, peak in the region between 1000 and 1200  $\text{cm}^{-1}$  representing the presence of CMC of PVP–CMC hydrogel which corresponds

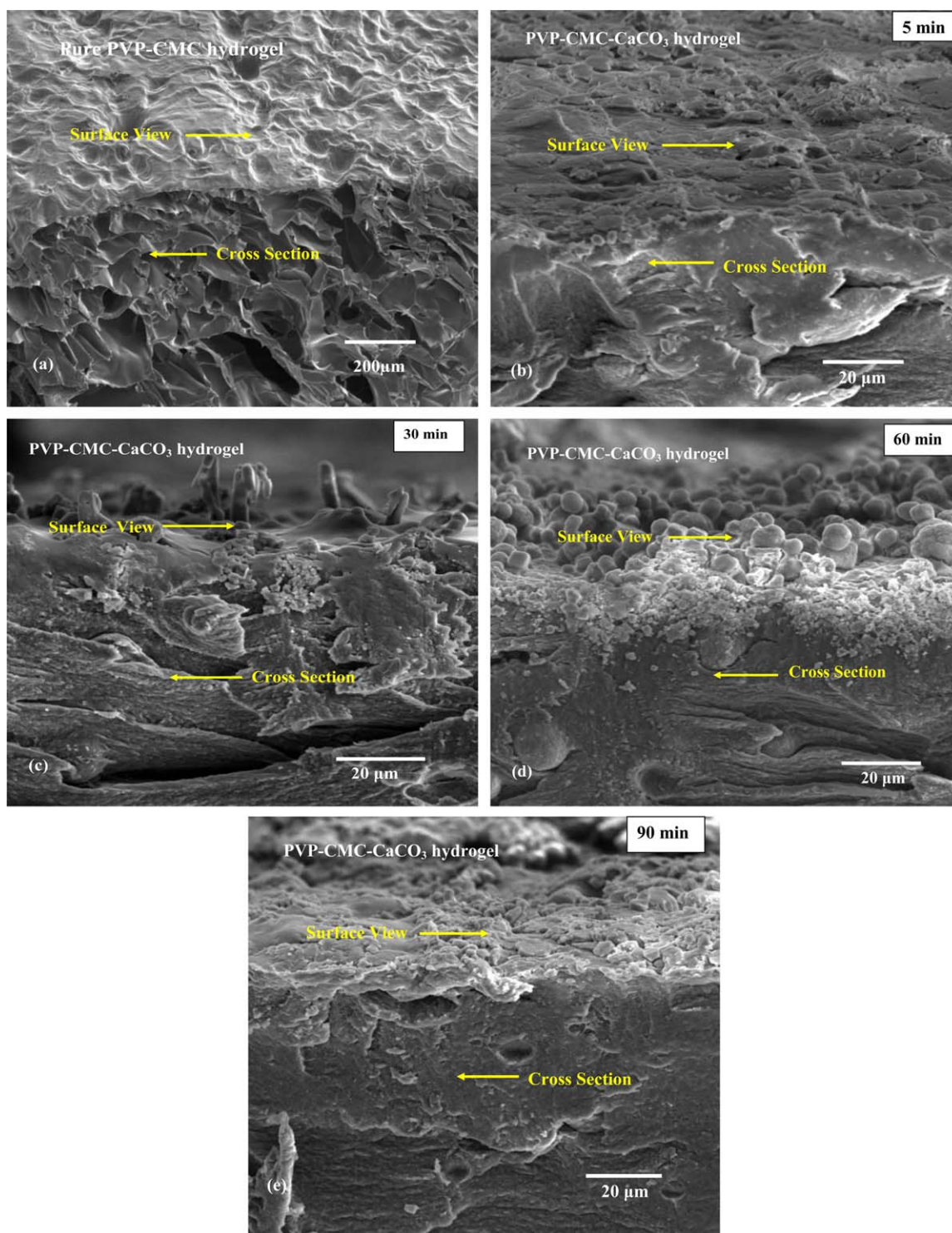


**Figure 2.** SEM micrographs of PVP-CMC hydrogels: (a) pure PVP-CMC; (b) biogenic mineralized (calcite) PVP-CMC hydrogels (duration 5 min); (c) biogenic mineralized (calcite) PVP-CMC hydrogels (duration 30 min); (d) biogenic mineralized (calcite) PVP-CMC hydrogels (duration 60 min); and (e) biogenic mineralized (calcite) PVP-CMC hydrogels (duration 90 min). [Color figure can be viewed in the online issue, which is available at [wileyonlinelibrary.com](http://wileyonlinelibrary.com).]

to the -C-O, C-CH stretching and CO and C-O-C bending of the glycoside ring of CMC<sup>3,27</sup>. Here, it is clearly visible from the spectrum that CMC related peak is present in nonmineralized hydrogel but during the process of mineralization and with the

increase in time, the intensity of CMC at particular wavenumber almost disappears, which confirms that there is deposition of calcium carbonate taking place within the hydrogel. Further, when considering the mineralized PVP-CMC hydrogel (a-h)

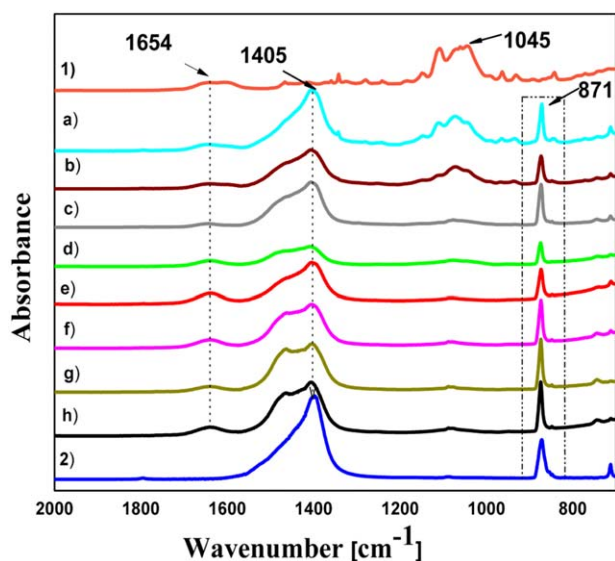


**Figure 3.** FTIR spectra of (1) PVP-CMC hydrogel, (2) pure  $\text{CaCO}_3$  and biomimetalized ( $\text{CaCO}_3$ ) PVP-CMC hydrogel in the order time of mineralization, i.e. 5, 10, 20, 30, 60, 90, 120, and 150 mins. [Color figure can be viewed in the online issue, which is available at [wileyonlinelibrary.com](http://wileyonlinelibrary.com).]

and pure  $\text{CaCO}_3$  strong absorption bonds related to  $\text{CO}_3^{2-}$  appear at  $1405\text{ cm}^{-1}$  and sharp peaks are noticed at  $871\text{ cm}^{-1}$ , which indicates the incorporation of  $\text{CaCO}_3$  into PVP-CMC hydrogel.<sup>7,8</sup>

#### Absorptivity of $\text{H}_2\text{O}$ and $\text{CaCO}_3$ within Hydrogels

The absorptivity of PVP-CMC hydrogel was studied for 150 min in the presence of water and mineral solutions (i.e.  $\text{Na}_2\text{CO}_3$  and  $\text{CaCl}_2$ ) to observe the  $\text{H}_2\text{O}$  uptake capacity as well as capacity to accumulate the biogenic mineral in the form of  $\text{CaCO}_3$  (as shown in Figure 5). It can be seen from the figure that the swelling or water uptake capacity of PVP-CMC hydrogel is faster and higher in quantity compared to ionic solutions that finally represent the uptake capacity of calcite (i.e.  $\text{CaCO}_3$ ). Hydrogels possess high water retention capacity.<sup>3</sup> There is an increase in polymeric interaction of fresh hydrogel related with the increase in time that leads to high sorption rate, and it finally leads to the water or minerals uptake potential of the hydrogel. The mineralized / calcite-based hydrogel is prepared using dry or water-swelled hydrogel film in ionic solutions wherein  $\text{Ca}^{+2}$  ions on the top layer act as nucleation sites and are slowly subjected to diffusion inside the membrane.<sup>10</sup> This leads to impregnation of calcite crystals in the cross-linking network and of the pores inside the hydrogel structure. However, the absorption rate of hydrogel would be expected from the increase in surface area with the increasing porosity of the hydrogels.<sup>25</sup> From Figure 4, it is clear that in the case of mineralized hydrogel, the rate of accumulation of  $\text{CaCO}_3$  within PVP-CMC hydrogel increases with time but there is not much difference observed in thickness of the mineralized hydrogel after 90 min though investigation continued until 150 min. Thus, we can consider that for biomineralization of PVP-CMC hydrogel (thickness 6 mm) with  $\text{CaCO}_3$ , 90 min is the optimum condition to reach the equilibrium state for diffusion of ionic salts within the matrix to fill the pores of the hydrogel. After 90

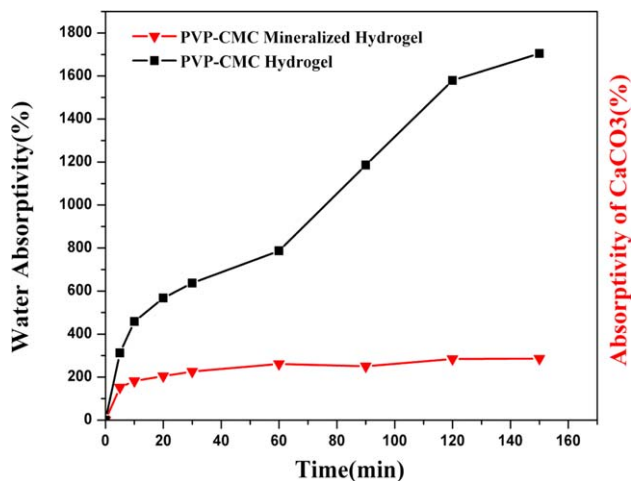


**Figure 4.** Absorption behavior of PVP-CMC hydrogel in presence of water and ionic solutions. [Color figure can be viewed in the online issue, which is available at [wileyonlinelibrary.com](http://wileyonlinelibrary.com).]

min, the biomimetic mineralization process continued but the  $\text{CaCO}_3$  crystal formation occurs on the surface of hydrogel which is ascertained by Figures 2(c,d,e).

#### Viscoelastic Properties of Hydrogels

The viscoelastic properties of PVP-CMC hydrogel of fresh (before dry sample), water swollen (swelled in water for 5 to 150 min) and mineralized (mineralized in ionic salt solution for 5–150 min) hydrogel samples were measured at room temperature. Figure 5 reveals the typical dynamic viscoelastic properties of 90 min swelled and mineralized (filled with  $\text{CaCO}_3$ ) PVP-CMC hydrogels as a function of angular frequency ( $\omega$ ). In the figure, the storage modulus ( $G'$ ) and loss modulus ( $G''$ ) of these hydrogels are compared with those of fresh PVP-CMC hydrogel, because a gel (elastic solid) property can be defined based

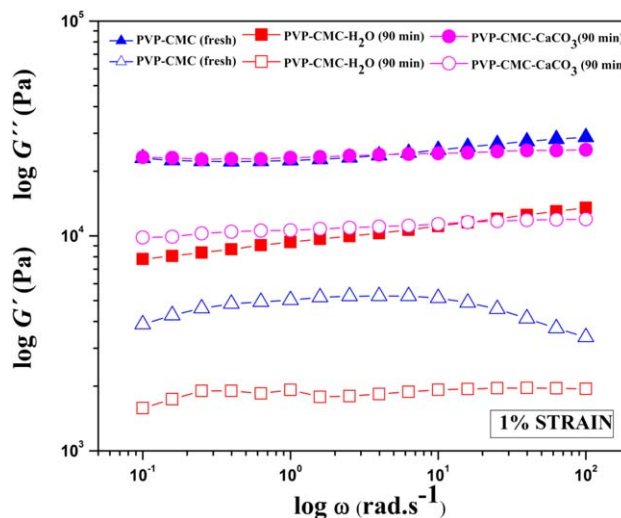


**Figure 5.** Storage modulus ( $G'$ , filled symbol) and loss modulus ( $G''$ , open symbol) as function of angular frequency ( $\omega$ ) at  $28^\circ\text{C}$  and 1% strain for fresh (before drying), swelled in water (90 min) and mineralized with  $\text{CaCO}_3$  (90 min) PVP-CMC hydrogels. [Color figure can be viewed in the online issue, which is available at [wileyonlinelibrary.com](http://wileyonlinelibrary.com).]

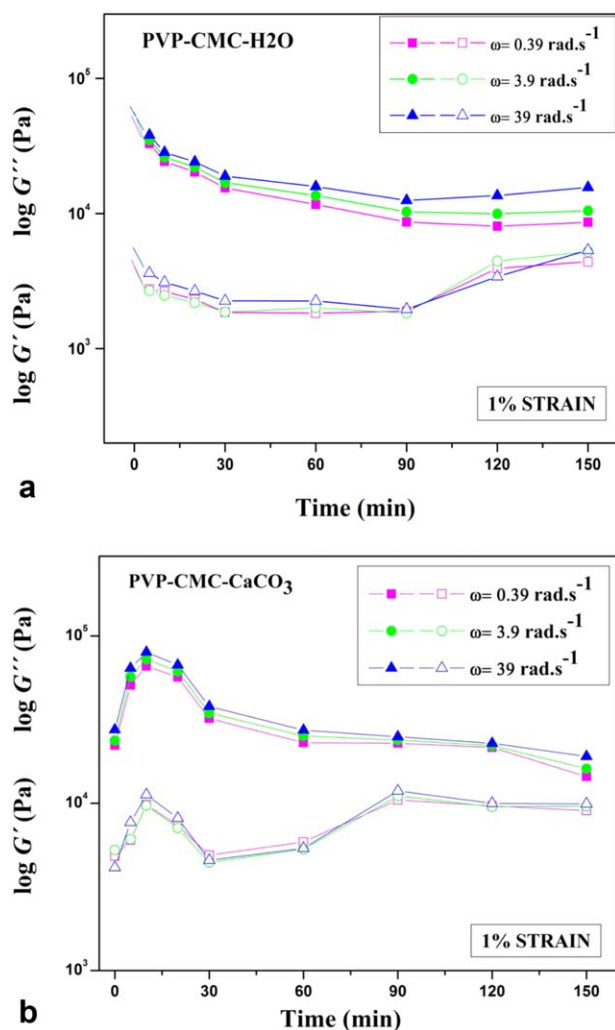


**Figure 6.** (a) Effect of swelling time (0–150 min) on storage modulus ( $G'$ , filled symbol) and loss modulus ( $G''$ , open symbol) as a parameter of angular frequency ( $\omega$ ) of 0.39, 3.9, and 39  $\text{rad s}^{-1}$  for water swelled PVP–CMC hydrogel. (b) Effect of swelling time (0–150 min) on storage modulus ( $G'$ , filled symbol) and loss modulus ( $G''$ , open symbol) as a parameter of angular frequency ( $\omega$ ) of 0.39, 3.9, and 39  $\text{rad s}^{-1}$  for mineralized ( $\text{CaCO}_3$ ) PVP–CMC hydrogel. [Color figure can be viewed in the online issue, which is available at [wileyonlinelibrary.com](http://wileyonlinelibrary.com).]

on the concept that the storage modulus ( $G'$ ) is dominant in the gel phase whereas the loss modulus ( $G''$ ) is dominant in the sol phase.<sup>28,29</sup> As can be seen in Figure 5, in case of fresh, swelled, and mineralized hydrogels the values of  $G'$  are higher than  $G''$  across the wide range of angular frequency ( $\omega$ : 0.1–100  $\text{rad s}^{-1}$ ), and dependence of these moduli on  $\omega$  is not high, which is characteristic for cross-linked hydrogels. It is also noticeable that the difference in values of  $G'$  and  $G''$  in mineralized hydrogel is not much compared to viscoelastic nature of fresh and swelled hydrogel although both moduli of mineralized hydrogel are higher than those of swelled hydrogel, which seems to confirm that the presence of  $\text{CaCO}_3$  within the PVP–CMC hydrogel enhances the cross-linkage number within the hydrogel matrix and then induces the increase of viscous nature. The elastic behavior of hydrogel shows its influences compared to

the viscous nature. Moreover all the hydrogels exhibited the linear curve which is also confirmed by typical characteristics for cross-linked gels or solid materials.<sup>7,8,28,29</sup> The results presented in Figure 5, also proved that there is not much difference in elastic properties of fresh and 90 min mineralized hydrogels but the values of elastic properties is decreased in the case of swelled hydrogel because of uptake of water (as shown in Figure 4) within the hydrogel matrix.

Relationships between  $G'$  and  $G''$  and swelling or mineralizing time as a parameter of angular frequency ( $\omega$ : 0.39, 3.9, and 39  $\text{rad s}^{-1}$ ) are shown for swelled hydrogels and mineralized ones in Figures 6(a,b), respectively. It can be seen from the figures that even though the swelled hydrogel decreases its elastic property ( $G'$ ) with time monotonously because of the incorporation of water into the pores of three-dimensional cross-linked PVP–CMC hydrogel [Figure 6(a)], the viscous property ( $G''$ ) of this hydrogel seems to be changed with swelling time as  $G'$  except the materials after long time swelling.

The mineralized/calcite-filled hydrogel [Figure 6(b)] show very different behavior form to that of the swelled hydrogel at shorter mineralization time, that is, after both moduli reach the maximum values and then the values decrease gradually after short time. Here, it is essential to mention that irrespective of changes in angular frequencies at 1% strain the  $G'$  and  $G''$  values of swelled and mineralized PVP–CMC hydrogel showed the same trend of viscoelastic nature [Figures 6(a,b)]. Though, the swelled hydrogel has been examined at different time intervals, the 90-min swelled samples exhibited mostly the same value of storage modulus ( $G'$ ) at different angular frequencies ( $\omega = 0.39$ , 3.9, and 39  $\text{rad s}^{-1}$ ). Similarly, the 90 min mineralized hydrogel also exhibited the same values at different angular frequencies ( $\omega = 0.39$ , 3.9, and 39  $\text{rad s}^{-1}$ ) regardless of  $G'$  and  $G''$ . Therefore, it can be predicted that 90 min is the optimum duration for performing the biomineralization process following the liquid diffusion technique to prepare calcite-filled PVP–CMC hydrogel at room temperature when thickness of fresh hydrogel is 6 mm.

The effect of water uptake time and mineralization duration on complex viscosity ( $\eta^*$ ) as a parameter of angular frequency ( $\omega$ ) are shown for water swelled PVP–CMC hydrogel as well as for  $\text{CaCO}_3$ -filled PVP–CMC hydrogel in Figures 7(a,b), respectively. As can be seen from Figure 7(a), the PVP–CMC hydrogel showed linear complex viscosity ( $\eta^*$ ) irrespective of different angular frequencies ( $\omega = 0.39$ , 3.9, and 39  $\text{rad s}^{-1}$ ) and becoming soft when swelled from dry PVP–CMC hydrogel. Moreover, no sharp changes occurred within the internal cross-linking structure of PVP–CMC hydrogel. On the other hand, it has been noticed that there is no physical difference observed within the  $\text{CaCO}_3$ -filled mineralized hydrogel, either the liquid diffusion mineralization process is initiated using dry or freshly prepared hydrogel. Thus, the effect of complex viscosity ( $\eta^*$ ) on mineralized PVP–CMC hydrogel has been compared with fresh hydrogel. It can be seen from Figure 7(b) that regardless of angular frequencies ( $\omega = 0.39$ , 3.9, and 39  $\text{rad s}^{-1}$ ) and at the beginning, approximately up to 10 min the values of complex viscosity ( $\eta^*$ ) are increased because of uptake of  $\text{CaCO}_3$  within

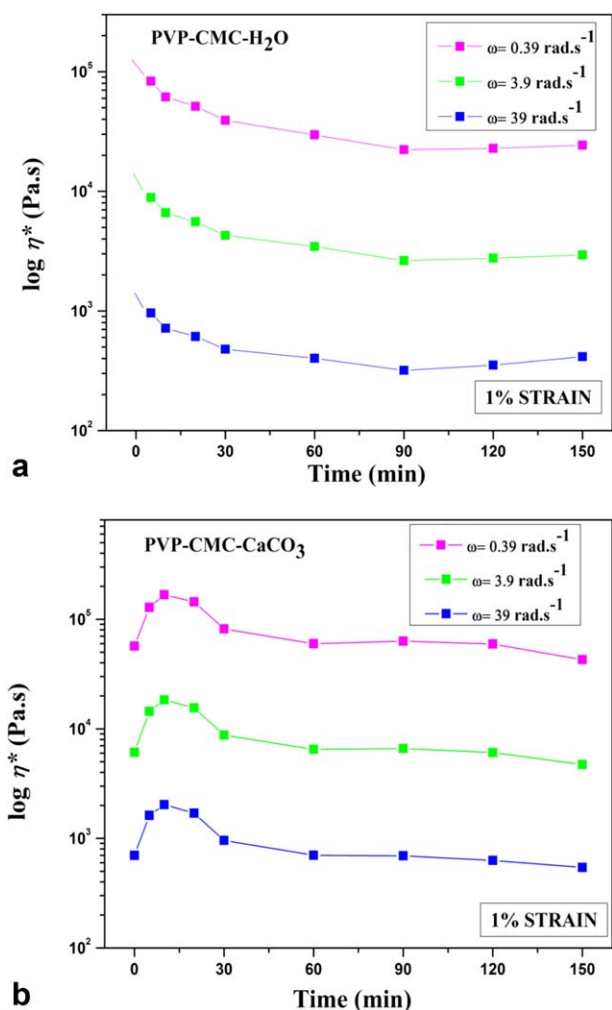


**Figure 7.** (a) Effect of time on complex viscosity ( $\eta^*$ ) as a parameter of angular frequency ( $\omega$ ) for water swelled PVP-CMC hydrogel. (b) Effect of time on complex viscosity ( $\eta^*$ ) for mineralized PVP-CMC hydrogel. [Color figure can be viewed in the online issue, which is available at [wileyonlinelibrary.com](http://wileyonlinelibrary.com).]

the three-dimensional cross-linked structure of PVP-CMC hydrogel [see Figure 2(a)] and when the pore of PVP-CMC hydrogels are saturated with CaCO<sub>3</sub>, the values of complex viscosity ( $\eta^*$ ) start to decrease from 30 min mineralization time, thereafter it shows a steady linear value of complex viscosity ( $\eta^*$ ) for the case of mineralized PVP-CMC hydrogel. The effect of time on complex viscosity ( $\eta^*$ ) is also attributed to the result of CaCO<sub>3</sub> absorption behavior of PVP-CMC hydrogel (as shown in Figure 4).

The linear viscoelastic properties of frequency sweep experiment for minimum duration (5 min) and maximum duration (150 min) swelled in water and mineralized PVP-CMC hydrogels are depicted in Figures 8(a,b), respectively, where storage modulus ( $G'$ , filled symbol) and loss modulus ( $G''$ , open symbol) are shown as a function of angular frequency ( $\omega$ : 0.1–100 rad s<sup>-1</sup>) at 28°C with 1% strain. These figures show more or less similar trends of viscoelastic behavior for both hydrogels that indicate the stable internal cross-linking structure of PVP-CMC hydrogel matrix.

Tan  $\delta$  of swelled (5 and 150 min) and mineralized (5 and 150 min) hydrogel samples as a function of angular frequency ( $\omega$ ) are depicted in Figure 9(a). It can be seen from the figure that Tan  $\delta$  of the samples of 150 min swelled or mineralized hydrogel are higher than that of 5 min swelled or mineralized ones over whole range of angular frequency, and at initial frequency range the Tan  $\delta$  remained steady and then gradually decreased when the PVP-CMC hydrogel samples are swelled or mineralized up to 150 min, whereas, for the case of 5 min swelled or mineralized hydrogel the Tan  $\delta$  is gradually decreased and then increased slightly. From these results it can be said that the change from elastic to viscous nature of both swelled and mineralized hydrogels may be influenced strongly by the swelling or mineralization time. In order to clarify the dependence of

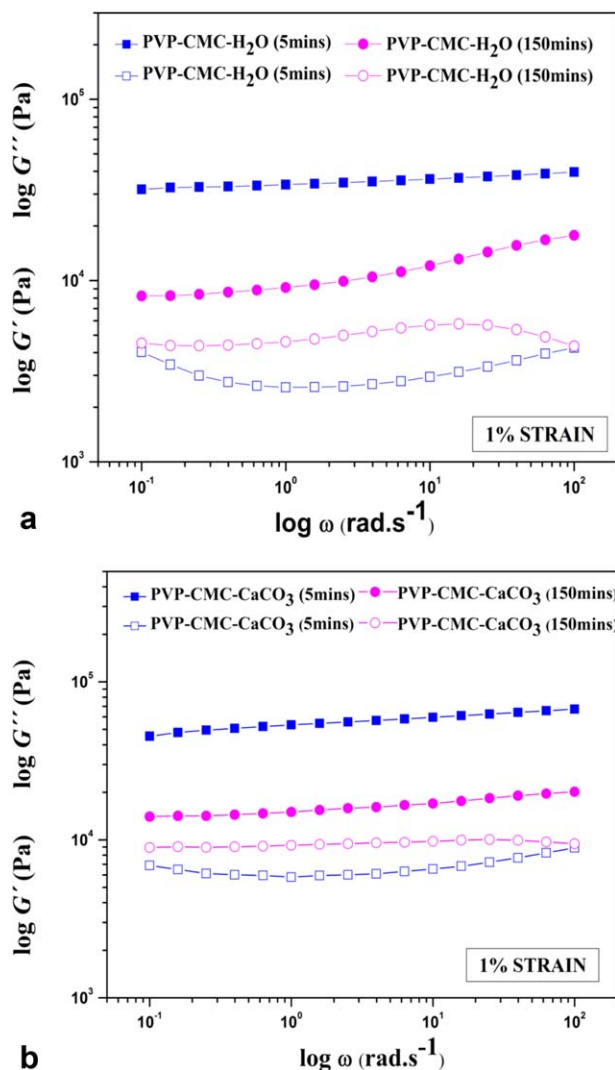


**Figure 8.** (a) Comparison of storage modulus ( $G'$ , filled symbol) and loss modulus ( $G''$ , open symbol) between water swelled PVP-CMC hydrogel of 5 min swelling time and that of 150 min one as a function of angular frequency ( $\omega$ ). (b) Comparison of storage modulus ( $G'$ , filled symbol) and loss modulus ( $G''$ , open symbol) between mineralized (CaCO<sub>3</sub>) PVP-CMC hydrogel of 5 min mineralizing time and that of 150 min one as a function of angular frequency ( $\omega$ ). [Color figure can be viewed in the online issue, which is available at [wileyonlinelibrary.com](http://wileyonlinelibrary.com).]

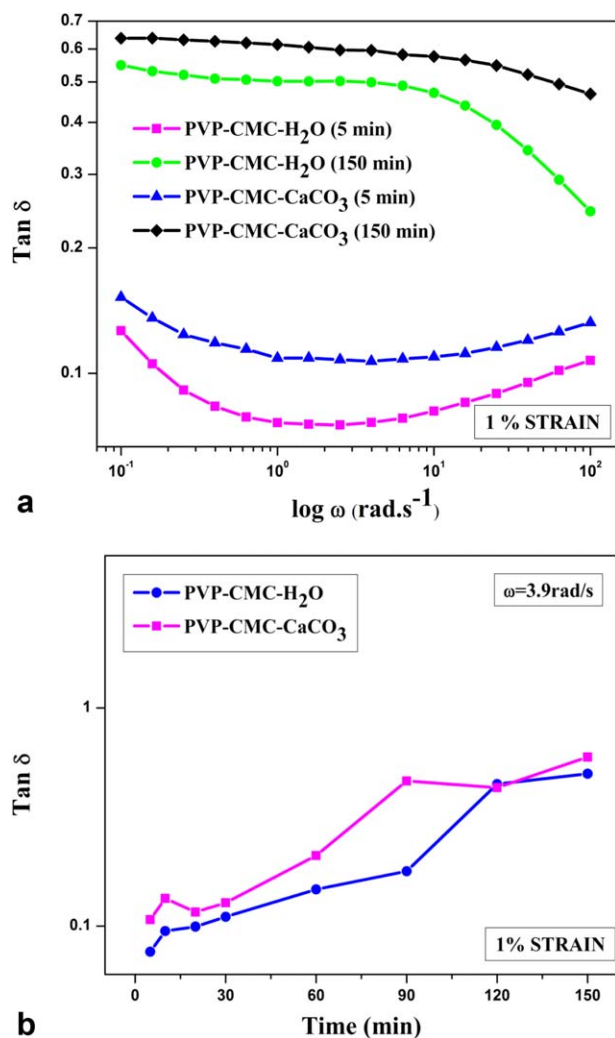


**Figure 9.** (a) Tan  $\delta$  as a function of angular frequency ( $\omega$ ) for swelled (5 and 150 min) and mineralized hydrogels (5 and 150 min). (b) Tan  $\delta$  as a function of swelling or mineralization time for swelled and mineralized hydrogels. [Color figure can be viewed in the online issue, which is available at [wileyonlinelibrary.com](http://wileyonlinelibrary.com).]

viscoelastic nature on the time, the relationship between Tan  $\delta$  and time of swelled and mineralized hydrogel at the angular frequency of 3.9 rad/s is shown in Figure 9(b). It is obvious from the figure that Tan  $\delta$  of both hydrogels increases with the increase of swelling or mineralization time. It does not increase smoothly, which confirms that both hydrogels change from elastic nature to viscous one with the increase of time.

## CONCLUSIONS

In this work, PVP-CMC hydrogel has been used as an extracellular matrix for biomimetic biomineralization study where the surfaces as well as pores were filled with CaCO<sub>3</sub>. Finally a regenerated and functionalized hydrogel membrane, which would be biogenic and bioactive for medical applications like bone tissue repairing, bone regeneration, tissue replacement, dental plaque, etc., has been developed. Concerning the advantage of using the PVP-CMC hydrogel film, primarily, this hydrogel was invented

at our laboratory, possible to be prepared in any size, shape, and thickness, and no chemical cross-linking agent was used. It is transparent, flexible, and hydrophilic in nature and moreover, it is possible to use it for biomineralization in fresh, dry, and also in swelled form. Thus, when liquid diffusion technique was implemented for the deposition of CaCO<sub>3</sub> within the PVP-CMC hydrogel matrix which showed an excellent absorptivity, good organic and inorganic interaction and finally a calcite-based new biomaterial termed as PVP-CMC-CaCO<sub>3</sub> or calcite-based PVP-CMC hydrogel was formed. This new material showed very stable and uniform viscoelastic properties maintaining its gel properties.

## ACKNOWLEDGMENTS

The authors are thankful for the support of Research and Development for Innovation Operational Program co-funded by the European Regional Development Fund (ERDF) and national budget of the Czech Republic within the framework of the Centre of Polymer Systems project (reg. number: CZ.1.05/2.1.00/03.0111) and the support of the “Education for Competitiveness” Operational Program co-funded by the European Social Fund (ESF) and the national budget of the Czech Republic, within the “Advanced Theoretical and Experimental Studies of Polymer Systems” project (reg. number: CZ.1.07/2.3.00/20.0104).

## REFERENCES

- Kuang, M.; Wang, D.; Gao, M.; Hartmann, J.; Mohwald, H. *Chem. Mater.* **2005**, *17*, 656.
- Zhuwei, D.; Cuixiang, L.; Haoran, L.; Dingjie, L. *Chin. J. Chem.* **2009**, *27*, 2237.
- Roy, N.; Saha, N.; Kitano, T.; Saha, P. *J. Appl. Polym. Sci.* **2010**, *117*, 1703.
- Saha, N.; Saari, A.; Roy, N.; Kitano, T.; Saha, P. *J. Biomater. Nanobiotechnol.* **2011**, *2*, 85.
- Saha, P.; Saha, N.; Roy, N. “Hydrogel Wound Covering” *Czech Pat. no: 302405, Czech Republic*.
- Roy, N.; Saha, N.; Kitano, T.; Saha, P. *Carbohydr. Polym.* **2012**, *89*, 346.
- Saha, N.; Shah, R.; Vyroubal, R.; Kitano, T.; Saha, P. *Novel Trends in Rheology V Book Series: AIP Conference Proceedings 2013*; 1526, 292. ISSN: 0094-243X, ISBN: 978-073541151-7.
- Saha, N.; Vyroubal, R.; Shah, R.; Kitano, T.; Saha, P. *Novel Trends in Rheology V Book Series: AIP Conference Proceedings 2013*; 1526, 301, ISSN: 0094-243X, ISBN: 978-073541151-7.
- Olderøy, M.; Xie, M.; Andreassen, P. J.; Strand, L. B.; Zhang, Z.; Sikorski, P. *J. Mater. Sci. Mater. Med.* **2012**, *23*, 1619.
- Rauch, M. W.; Dressler, M.; Scheel, H.; Opdenbosch, D. V.; Zollfrank, C. *Eur. J. Inorg. Chem.* **2012**, 5192.
- Yang, X.; Akhtar, S.; Rubino, S.; Leifer, K.; Hilborn, J.; Ossipov, D. *Chem. Mater.* **2012**, *24*, 1690.
- Nonoyama, T.; Ogasawara, H.; Tanaka, M.; Higuchi, M.; Kinoshita, T. *Soft Matter.* **2012**, *8*, 11531.



13. Huang, J.; Liu, G.; Song, C.; Saiz, E.; Tomsia, P. A. *Chem. Mater.* **2012**, *24*, 1331.
14. Aizenberg, J. *Adv. Mater.* **2004**, *16*, 1295.
15. Carrillo, N. A.; Quitral, V. P.; Pedram, Y. M.; Arias, L. *J. Eur. Polym. J.* **2010**, *46*, 1184.
16. Ni, M.; Ratner, D. B. *Surf. Interface Anal.* **2008**, *40*, 1356.
17. Ma, Y.; Feng, Q. *J. Solid State Chem.* **2011**, *184*, 1008.
18. Xia, Y.; Gu, Y.; Zhou, X.; Xu, H.; Zhao, X.; Yaseen, M.; Lu, R. *J. Biomacromolecules* **2012**, *13*, 2299.
19. Smith, E. A.; Li, H.; Keene, E. C.; Seh, Z. W.; Estroff, L. A. *Adv. Funct. Mater.* **2012**, *22*, 2891.
20. Zhang, F. J.; Yang, X. G.; Zhuang, Y.; Guo, K. K.; Wang, M. J.; Wei, W. F. *J. Cent. South Univ.* **2012**, *19*, 1802.
21. Li, H.; Estroff, A. L. *CrystEngComm*, **2007**, *9*, 1153.
22. Kim, Y. S.; Lee, C. S. *J. Appl. Polym. Sci.* **2009**, *113*, 3460.
23. Guzun, S. A.; Stroescu, M.; Jinga, S.; Jipa, I.; Dobre, T.; Dobre, L. *Ultrason. Sonochem.* **2012**, *19*, 909.
24. Sinha, A.; Agrawal, S.; Nayar.; Das, K. S.; Ramachandrarao, P. *J. Mater. Synth. Process.* **2002**, *10*, 149.
25. Mahdavinia, R. G.; Mousavi, B. S.; Karimi, F.; Marandi, B. G.; Garabaghi, H.; Shahabvand, S. *eXPRESS Polym. Lett.* **2009**, *5*, 279.
26. Junji, W.; Mitsuru, A. *Biomacromolecules* **2006**, *7*, 3008.
27. Pasqui, D.; Torricelli, P.; Cagna, M. D.; Fini, M.; Barbucci, R. *J. Biomed. Mater. Res. A* **2013**, *00A*, 00,1.
28. Zhang, J. T.; Bhat, R.; Jandt, K. D. *Acta Biomater.* **2009**, *5*, 488.
29. Fathi, M.; Entezami, A. K.; Pashaei-Asl, R. *J. Polym. Res.* **2013**, *20*, 125, 10.1007/s10965-013-0125-5.